JUSTC

Review

http://justc.ustc.edu.cn

Received: November 22, 2022; Accepted: February 06, 2023

Chiral inorganic nanostructures for theranostics

Yaxin Wang*, Zhi Tong*, Yajie Zhou, Xueru Guo, Mingjiang Zhang, Shanshan Zhao, and Taotao Zhuang ✉

Department of Chemistry, and Hefei National Research Center for Physical Sciences at the Microscale, University of Science and Technology of China, Hefei 230026, China

* These authors contributed equally to this work

✉Correspondence: Taotao Zhuang, E-mail: tzhuang@ustc.edu.cn

Graphical abstract

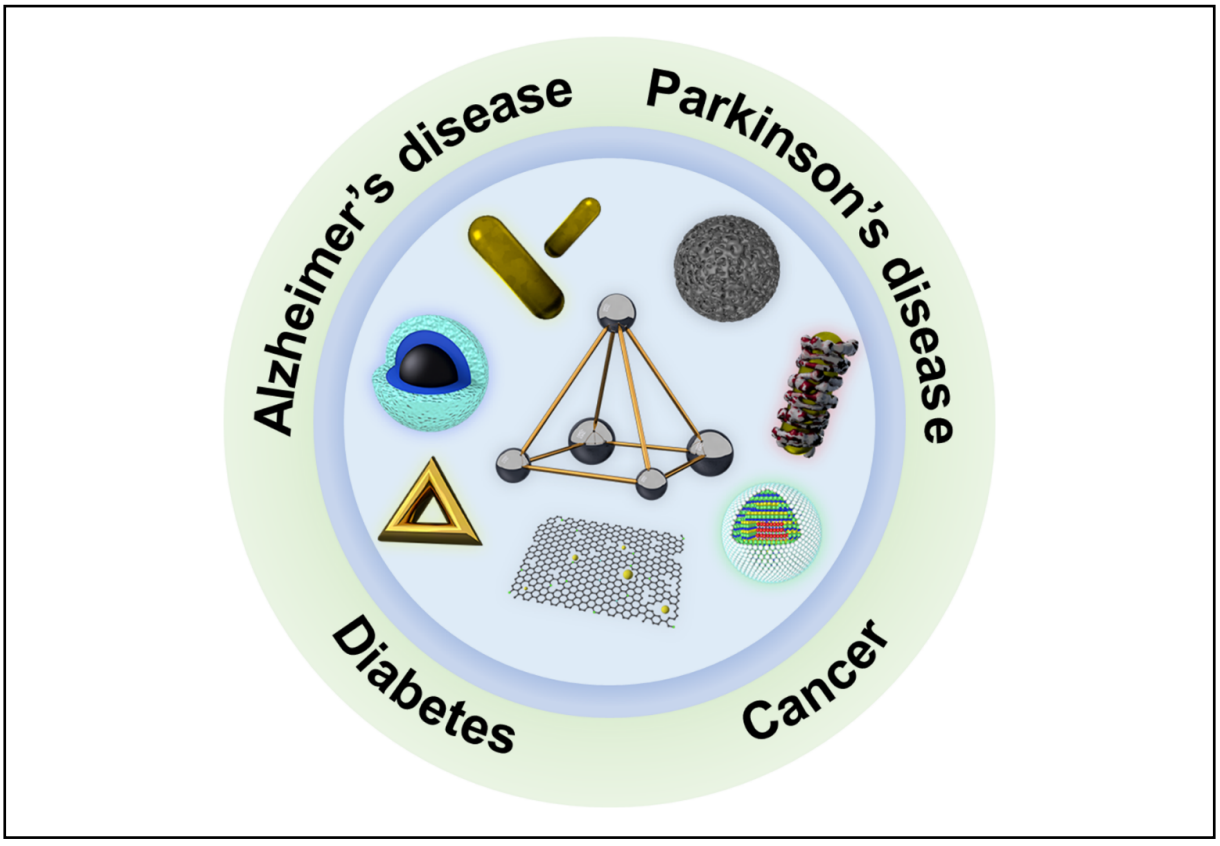

Schematic illustration of applications in clinical diseases using chiral inorganic nanostructures.

Public summary

- We summarize several types of inorganic chiral nanostructures, including metals, semiconductors and carbon dots, that are promising for biological applications, especially clinical medicine.
- We present an in-depth discussion on their theragnostic functions for diabetes, Alzheimer's disease, Parkinson's disease and cancers.
- We declare that chiral materials are promising for improving the sensitivity of detection and enhancing the specificity of therapy compared with traditional inorganic nanomaterials.

Citation: Wang Y X, Tong Z, Zhou Y J, et al. Chiral inorganic nanostructures for theranostics. *JUSTC*, **2023**, 53(3): 0303. DOI: 10.52396/JUSTC-2022-0167

JUSTC

Review

http://justc.ustc.edu.cn

Received: November 22, 2022; Accepted: February 06, 2023

Chiral inorganic nanostructures for theranostics

Yaxin Wang*, Zhi Tong*, Yajie Zhou, Xueru Guo, Mingjiang Zhang, Shanshan Zhao, and Taotao Zhuang ✉

Department of Chemistry, and Hefei National Research Center for Physical Sciences at the Microscale, University of Science and Technology of China, Hefei 230026, China

* These authors contributed equally to this work

✉Correspondence: Taotao Zhuang, E-mail: tzhuang@ustc.edu.cn

Cite This: *JUSTC*, **2023**, 53(3): 0303 (13pp)

Read Online

Abstract: Inorganic chiral nanomaterials have attracted wide attention because of their superior physical properties and chiroptical activities. Great progress in chiral nanostructure preparation has been made, such as noble metals and semiconductors. In this review, we introduce several chiral nanomaterials with feasible biocompatibility and low cytotoxicity that are promising candidates for biological applications, and we focus on their preparation in terms of their circular dichroism (CD) effects and circular luminescence properties. Additionally, we summarize the working function of chiral nanostructures toward some common diseases with high prevalence, such as Alzheimer's disease (AD), Parkinson's disease (PD), diabetes and even cancers. The introduction of inorganic chirality will provide a novel way to diagnose and treat these diseases.

Keywords: inorganic chirality; nanostructure; theranostics; disease

CLC number: TB383.1 **Document code:** A

1 Introduction

Chirality exists extensively in nature and plays an extraordinarily essential role in biological systems[1]. Most biomolecules are chiral, and many biological processes also occur in chiral substances[2]. Chiral nanostructures have remarkable significance for many biological events, such as cellular metabolism, cell differentiation and cell apoptosis[3−6]. Subsets of chirality have been extensively studied before, especially inorganic chiral nanomaterials, including chiral plasmonic nanoparticles (NPs)[7], chiral semiconductor nanostructures[8], chiral nanocrystals[9], and chiral assemblies[4]. Different from traditional materials, chiral structures can exhibit better biochemical stability, lower toxicity and more biomechanical compatibility.

The applications of chiral materials have been widely dispersed in biology because of their incomparable properties. For example, Xu et al. reported a plasmonic chiroptical dimer whose chiroptical assemblies were controlled by cysteine (Cys) to recognize and quantize Cys enantiomers with different signals of CD spectrum[10]. An ATP-driven chiral system that can specifically identify ATP investigated by Liu et al. showed circularly polarized light (CPL) signals only when ATP interacted with achiral terpyridine-based Zn(II)[11]. In addition to detecting and sensing, chiral nanomaterials also affect the regulation of vital activities[5, 12−14]. Due to the difference in the absorption of left and right CPL[15], chiral nanomaterials could improve the selectivity, and thus, targeted interactions would occur between living cells and chiral molecules. Xia and Wang prepared chiral $Cu_{2-x}S$ nanocrystals (NCs) using chiral ligands and ligand exchange and then obtained NCs with mirror chiral signals, but D-$Cu_{2-x}S$ NCs showed three times higher cell uptake than L-NCs in HepG2 and HeLa cells, which possibly resulted from their higher affinity for the cell membrane of tumor cells[16]. Recently, Kuang and coworkers obtained gold (Au) particles with a maximal asymmetry factor (*g*-factor) up to 0.44 using CPL as the chiral generation source. These particles could regulate the maturation of immune cells, raising the possibility of tailoring immune responses within nanoscale chirality[17]. Furthermore, Kuang et al. also used L- or D-penicillamine (Pen) to modify Au particle films. The resulting films showed discrepant influences on cell growth and differentiation with opposite chiral signals[18]. Moreover, chiral nanostructures can also be used for photothermal therapy (PTT) and photodynamic therapy (PDT) by applying internal heating to tumor cells and producing more singlet oxygen, respectively. Xu and coworkers synthesized chiral molybdenum oxide (L/D-Cys-MoO_{3-x}) NPs by step-by-step reduction treatment of chiral cysteine molecules, and chiral MoO_{3-x} showed enhanced (ca. 30% improvement) PTT performance compared to their original counterparts[19]. Kuang and coworkers designed chiral cobalt superstructures (Co SS) with different morphologies to generate reactive oxygen, which resulted in excellent killing ability against gram-positive Staphylococcus aureus[20]. This review focuses on functional biofriendly chiral nanomaterials, including chiral metal nanocrystals, chiral semiconductor nanoparticles and chiral carbon dots (CDs). Chiral nanostructures possess some remarkable advantages, such as suitable biocompatibility, biochemical stability and long existence in vivo[21]. Regarding their applications in biology, different from other reviews, here, some noticeable diseases that can be detected or even cured by chiral nanomaterials will be introduced, such as diabetes, Alzheimer's disease (AD),

DOI: 10.52396/JUSTC-2022-0167

JUSTC, **2023**, 53(3): 0303

Parkinson's disease (PD), and cancers. Compared with traditional therapies such as surgery and lifelong medication, chiral substances not only exhibit appropriate biocompatibility but can also overcome poor targeting and enhance the therapeutic effect[22, 23].

2 Materials and methods

2.1 Chiral metal nanomaterials

Noble metals mainly refer to gold, silver and platinum group metals, which can be assembled into chirality. The surface plasmon effect of noble metals such as Au, silver, and platinum can significantly enhance the chiral signals of asymmetric nanostructures, leading to enhanced CD signals and high *g*-factor values. These asymmetric nanomaterials can be divided into chiral NPs with intrinsic chirality induced by chiral inducers, core-shell structures with chiral features, and chiral assemblies with superior structures. Various chiral inducers have been reported thus far[24], and in this section, we focus on the recent progress of induced chirality by chiral ligands, CPL, and assemblies with structural chirality using biomolecules (e.g., deoxyribonucleic acids (DNA), peptides, proteins) as templates, which have potential applications in biodetection and disease treatment. For instance, tumor cell recognition can also be achieved by recognizing biomarkers using aptamer-linked chiral NP components.

2.1.1 Monodisperse chiral metal NPs

In recent years, the synthesis of monodisperse chiral NPs with large *g*-factor values up to 10^{-1} by bottom-up synthesis has attracted much attention. Noble metal-based nanocubes[7, 17], nanorings[25], nanorods (NRs)[26–31], nanowires[32], and triangular nanoplates[33] have been developed with novel chiral properties lacking in achiral nanostructures. In 2018, Nam et al. synthesized chiral Au NPs with a high *g*-factor value up to 0.2 (Fig. 1a–d) using amino acids such as Cys and peptides such as glutathione (GSH) to control the handedness of Au nanocubes, successfully introducing molecular chirality into metal NPs[7]. In 2020, Liz-Marzán et al. prepared Au NRs with strong plasma activities, followed by depositing a helical-shaped Au shell on the nanorod surface using micelles (Fig. 1e–g), reaching a *g*-factor value of 0.22 (Fig. 1h). This micelle-guided mechanism can be extended to other systems, providing a simplified method for the fabrication of chiral structures[26]. In 2022, Xu et al. produced monodisperse chiral Au NPs with a *g*-factor value up to 0.44 (Fig. 1i–m) induced by chiral ligands under CPL irradiation. These highly asymmetric NPs were used to regulate the maturation of immune cells. Compared with right-handed NPs, the working efficiency of left-handed NPs was significantly enhanced, showing strong enantiomer selectivity and *g*-factor dependence. This method opened a new way for the applications of nanoscale chirality in immunology[17]. Subsequent in-depth research found that these chiral Au NPs also presented potential in applications of inducing apoptosis of cancer cells[34] and senescent cells[35].

2.1.2 Chiral assemblies

The variation in CD signals caused by the construction and destruction of chiral nanostructures using DNA origami technology[30, 36–38] provides a new method for detecting molecules such as reactive oxygen species[39], bovine serum albumin (BSA)[40], hydrogen sulfide[41], microRNA[36], and mycotoxin[42] both in vitro and in vivo. Structures are built through specific connections of biological molecules (such as chiral pyramids[36–38], propeller-like NRs[30], and core–satellite superstructures with Au NPs as the core[42]). The conformational changes in such a multiparticle combination cause structural damage apparent in the optical spectra, providing a more sensitive and more specific plasmon ruler in biological detection. In 2008, Alivisatos and colleagues created chiral pyramids, that is, DNA-topped Au nanospheres with different sizes (Fig. 2a, b). As each strand had a unique nanocrystal, it was possible to construct a highly asymmetric structure by placing different types of nanocrystals at each tip[43]. In 2014, Tang and coworkers researched the influence of different assembly methods on chirality, in which chiral Cys and Au NRs were intentionally assembled in typical end-to-end (EE) and side-by-side (SS) patterns. Conformationally modulated plasma CD enhancement was observed, and the result indicated that the enhanced conformational dependence of the plasma CD response was attributable to changes in the electromagnetic interaction between GNRS in the components[44]. In addition to the typical chiral signal changes[38], Kuang et al. designed pyramid structures to construct bimodal probes with CD signals and upconversion luminescence signs for biological detection. Chiroplasmonic pyramidal nanostructures, self-assembled from Au and upconverted NPs (UCNPs), were used to quantify microRNA in living cells (Fig. 2c), and the CD intensity had a lower limit of detection (LOD) than the upconverted luminous signal (Fig. 2d, e)[36]. In addition to bonding the upconverted luminescent material directly to a vertex of the tetrahedron, they also designed a chiral nanodevice consisting of nanoparticle tetrahedra centralized with UCNPs (Fig. 2f), in which the chiral component was used to induce autophagy while the UCNPs were used for visualization[37]. In addition, Au and silver heterodimer structures were constructed according to the antigen-antibody pairing principle (Fig. 2g)[45], and chiral core-shell satellite nanostructures (Fig. 2h)[42] and other chiral assemblies also showed excellent chiral optical activities, exhibiting notable potential applications in biological technology.

2.2 Chiral semiconductor NPs

Chiral semiconductor NPs have been spotlighted in recent years due to their tunable optical properties, leading to various applications, especially in biological sensors and detection[46]. The chiral generation of chiral semiconductor NPs is similar to that of metal NPs: (i) intrinsic chirality[47], (ii) chirality induced by chiral ligands[48], and (iii) chirality from assembly[49]. Among these, ligand exchange has attracted considerable attention for obtaining the expected QDs (quantum dots, a typical type of semiconductor NP).

He et al. prepared colloidal CdSe-dot/CdS nanorods (CdSe/CdS DRs) and further employed L- and D-Cys as ligands to generate water-soluble chiral CdSe/CdS DRs with tunable CPL, achieving an anisotropic factor (g_{lum}) value of 4.66×10^{-4}. The authors found that the CD and CPL activities

DOI: 10.52396/JUSTC-2022-0167
JUSTC, **2023**, 53(3): 0303

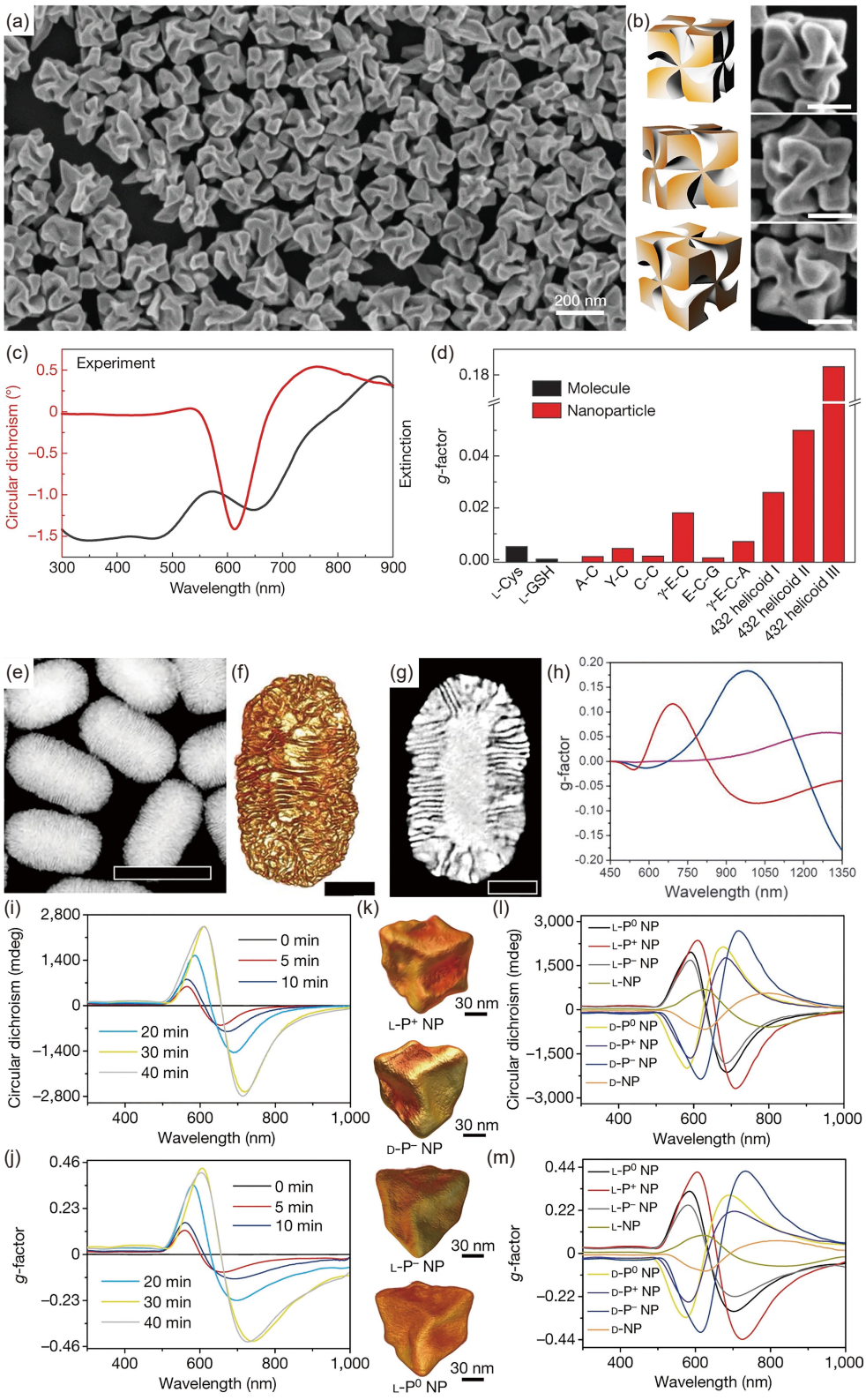

Fig. 1. (a) SEM image, (b) 3D models and corresponding SEM images (scale bars: 100 nm), and (c) experimental CD and extinction spectra of 432 helicoid III chiral NPs induced by L-cysteine. (d) *g*-factor comparison among 432 helicoid III, other NPs, and chiral molecules. Adapted with permission from Ref. [7]. Copyright 2018, Springer Nature. (e) HAADF-STEM image (scale bars: 200 nm), (f) 3D reconstructions (scale bars: 50 nm) and (g) orthoslices (scale bars: 50 nm) of chiral Au NRs. (h) *g*-factor spectra of chiral Au NRs with different sizes. Adapted with permission from Ref. [23]. Copyright 2020, the American Association for the Advancement of Science. (i) CD and (j) *g*-factor spectra of L-P$^+$ NPs exposed to laser irradiation for different durations. (k) TEM tomography images of L-P$^+$, D-P$^-$, L-P$^-$, and L-P^0 NPs. (l) CD and (m) *g*-factor spectra of synthesized chiral Au NPs. Adapted with permission from Ref. [16]. Copyright 2022, Springer Nature.

DOI: 10.52396/JUSTC-2022-0167
JUSTC, **2023**, 53(3): 0303

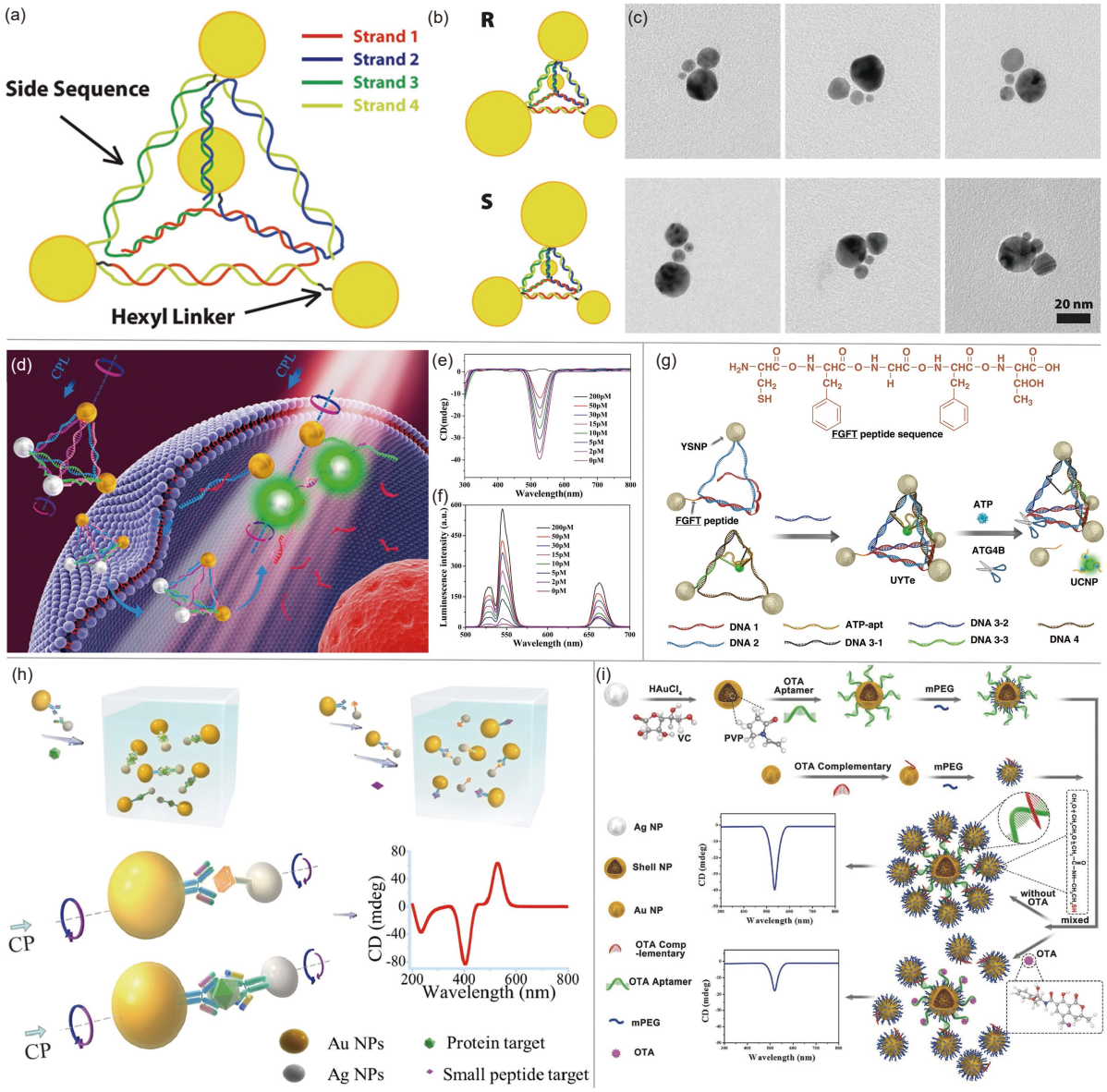

Fig. 2. (a) Structure of DNA-nanocrystal pyramids. (b) Schematic and (c) TEM images of chiral pyramids. Top row, R; bottom row, S. Adapted with permission from Ref. [40]. Copyright 2009, American Chemical Society. (d) Schematic illustration of the Au-UCNP pyramids for microRNA detection. (e) CD and (f) luminescence spectra of Au-UCNP pyramids. Adapted with permission from Ref. [33]. Copyright 2016, American Chemical Society. (g) Tetrahedron NPs centralized with UCNPs. Adapted with permission from Ref. [34]. Copyright 2018, American Chemical Society. (h) Schematic illustration of nanoparticle heterodimer assembly and its application in biological analysis. Adapted with permission from Ref. [41]. Copyright 2013, American Chemical Society. (i) Synthesis of shell core–Au satellite and detection of ochratoxin A based on chiral signal. Adapted with permission from Ref. [39]. Copyright 2018, Wiley-VCH.

were inhibited on account of the excess ligands (Fig. 3a–d). After a series of experiments, they observed that the CD and CPL signal intensities were closely related not only to their surface defects but also to the concentration of Cys (Fig. 3e–f)[50].

Later, Gun'ko et al. also utilized Cys to prepare aqueous-favoring chiral CdSe/CdS core/shell QDs via ligand exchange. In this research, the influences of the chiral ligand concentration and binding mode on the optical properties of chiral QDs were investigated in detail. With different concentrations of the ligands, the CD activities changed obviously; however, the dependence was nonlinear. With the addition of Cys, the CD signal intensities changed from enhanced to suppressed, whose changing trend was similar to the normal distribution function, and the optimal concentration of Cys was confirmed (Fig. 4g–h). ^{1}H and ^{13}C nuclear magnetic resonance (NMR) spectroscopy analyses and Fourier transform infrared (FTIR) spectroscopy were used to explain the decrease in the *g*-factor (Fig. 3i–k), and they demonstrated that the binding mode between the Cys and the QDs transformed as the content of Cys increased[51].

In recent years, with the progress of QD surface modification, the stability and water solubility of QDs have been improved, enabling their use in biological applications. Hua Kuang's group mixed odium citrate in the absence of oxygen with $CuCl_2$, followed by heating with thiourea and D-/L-Pen,

DOI: 10.52396/JUSTC-2022-0167
JUSTC, **2023**, 53(3): 0303

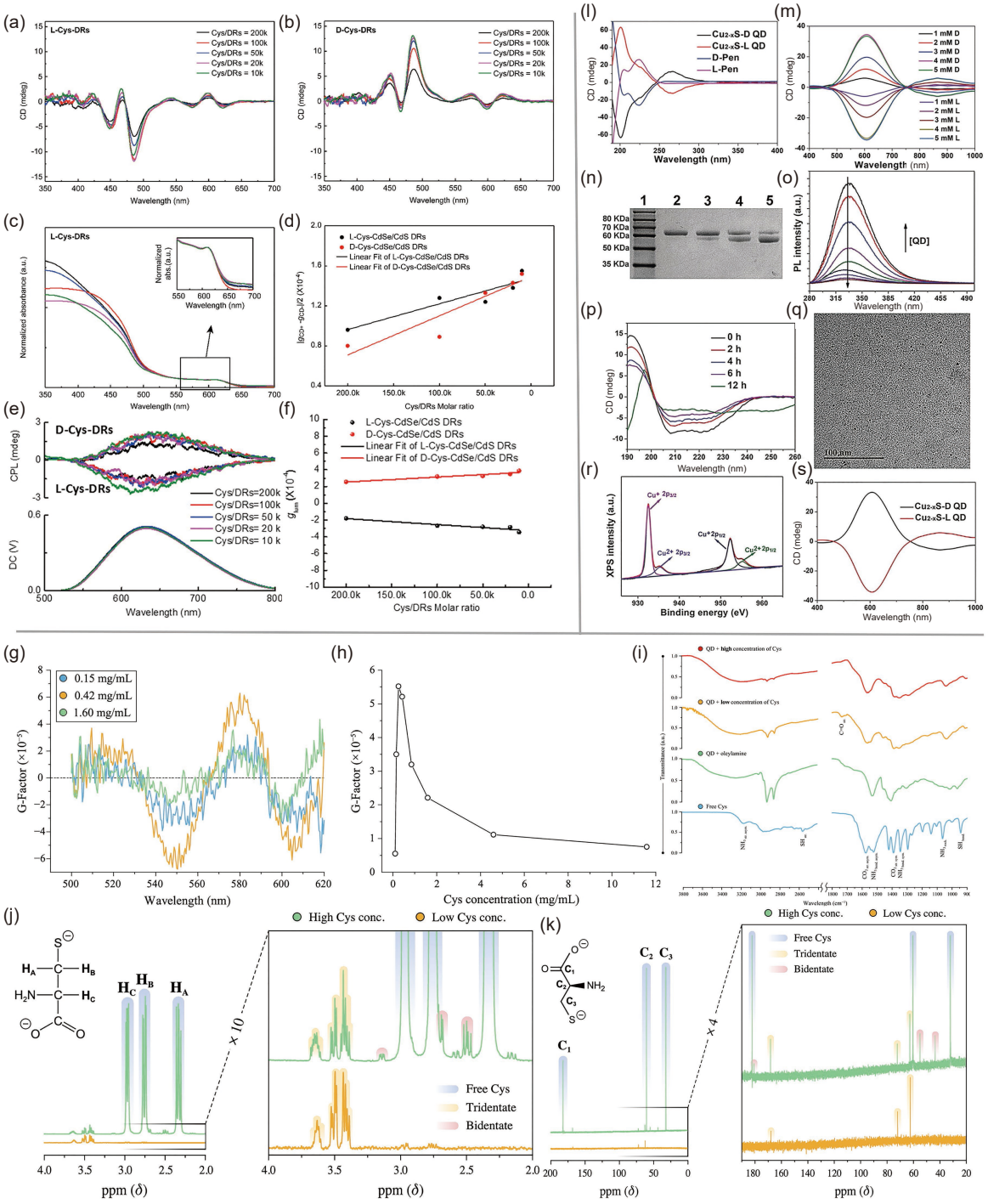

Fig. 3. (a) CD spectra of L-cysteine-DRs and (b) D-cysteine-DRs. (c) UV/vis spectra of L-cysteine-DRs with different cysteine/DR ratios. (d) Illustration of the relationship between the *g*-factor of CdSe/Cds DRs and the ratio of cysteine/DRs. (e) CPL spectra and (f) g_{lum} values of L- and D-cysteine-DRs with different cysteine/DR ratios. Adapted with permission from Ref. [46]. Copyright 2018, American Chemical Society. (g) g_{lum} of chiral CdSe/CdS QDs with different concentrations of cysteine. (h) The relationship between g_{lum} and the concentration of cysteine at 605 nm. (i) FTIR spectra of QDs and QDs with cysteine or organic ligands. (j) ^{1}H NMR spectra and (k) ^{13}C NMR spectra of QDs. Adapted with permission from Ref. [47]. Copyright 2019, American Chemical Society. (l) CD spectra of L-/D-pen and the chiral QDs. (m) CD spectra of QDs with various concentrations of chiral Pen. (n) Illustration of the influence of L-QDs on the cleavage of BSA under different light conditions. Lane 1, molecular marker; lane 2, BSA; lane 3, BSA + RCP; lane 4, BSA + LP; lane 5, BSA + LCP. (o) PL spectra of BSA with different concentrations of L-QDs. (p) CD spectra of photolysis of BSA at different reaction times. (q) TEM image of L-QDs after interacting with BSA. (r) XPS Cu 2p spectrum of l-QDs after the reaction. (s) CD spectra of the QDs after the cleavage reaction. Adapted with permission from Ref. [48]. Copyright 2019, Wiley-VCH.

to fabricate chiral $Cu_{2-x}S$ QDs with a high g_{lum} value of 0.01. The CD signals from the QDs were distinguished from the intrinsic CD peak of L- and D-Pen due to the emergence of new peaks for the QDs, owing to the interaction of Pen and QDs (Fig. 3l). Moreover, the QDs were applied to the photocatalytic cleavage of BSA. They revealed that the L-QDs could

DOI: 10.52396/JUSTC-2022-0167
JUSTC, **2023**, 53(3): 0303

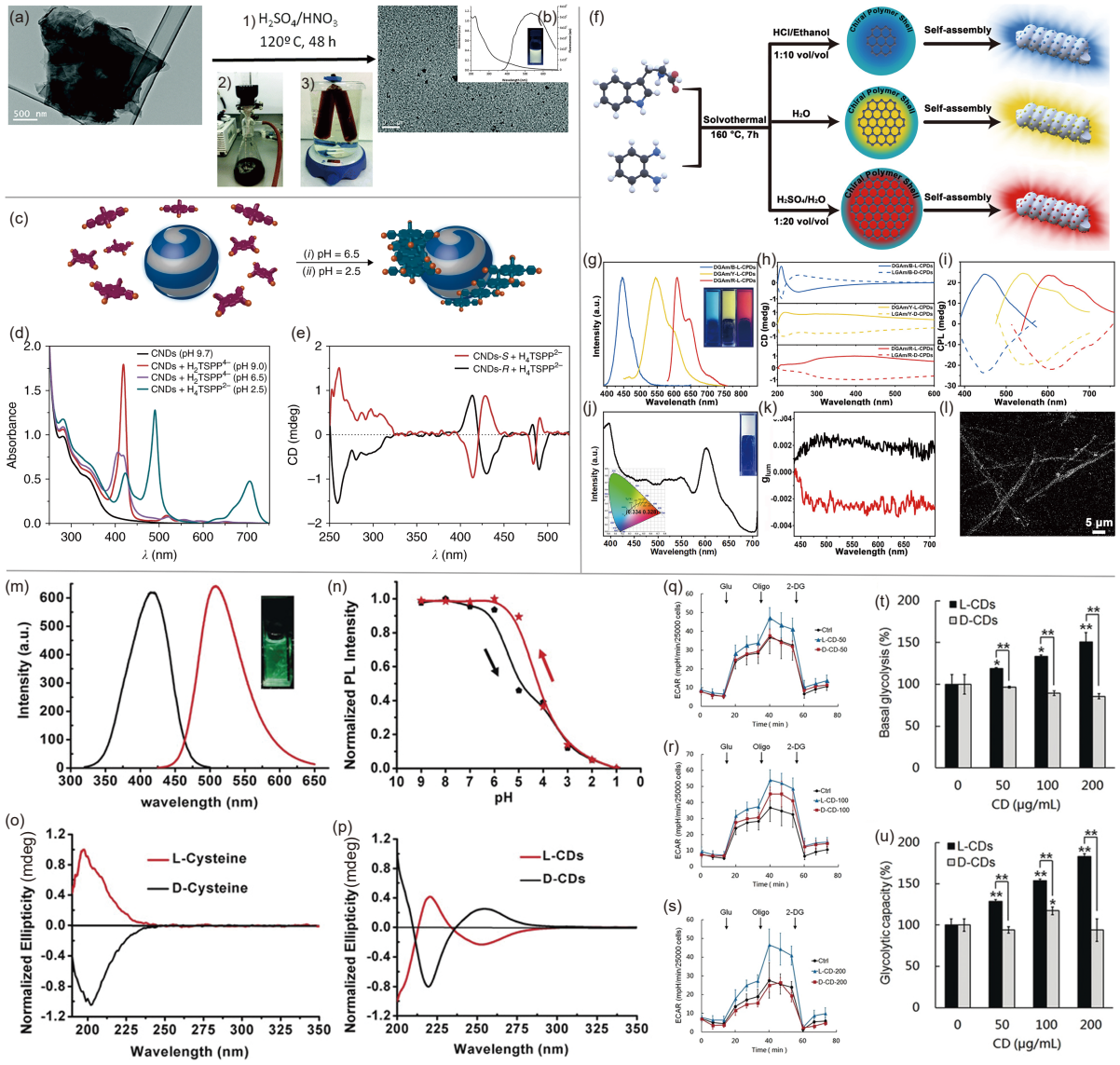

Fig. 4. (a) Illustration of the fabrication of chiral GQDs by a three-step approach. (b) UV–vis and FL spectra of GQDs. Adapted with permission from Ref. [50]. Copyright 2016, the Royal Society of Chemistry. (c) Illustration of chiral CDs as supramolecular templates. (d) UV–vis spectra of CDs and CDs with H_nTSPP^{m-} at different pH values. (e) ECD spectra of L- and D-CDs with H_nTSPP^{m-}. Adapted with permission from Ref. [51]. Copyright 2018, Springer Nature. (f) Illustration of the preparation approach for multicolor-emitting chiral CDs. (g) PL spectra of the three types of CDs. (h) CD spectra and (i) CPL of the three CDs capped with gels. (j) Illustration of the CIE value of white PL. (k) g_{lum} values of L- and D-CDs. (l) Laser scanning confocal microscope image of white luminescent colloid. Adapted with permission from Ref. [52]. Copyright 2021, Wiley-VCH. (m) PL spectra of the excitation spectrum (black line) and emission spectrum (red line) of L-CDs. (n) Illustration of the relationship of the intensity of the L-CD PL emission. (o) CD spectra of L- and D-Cys and (p) L- and D-CDs. (q–u) Illustration of the influence of chiral CDs on mitochondrial respiration on behalf of the oxygen consumption rate (OCR) of T24 cells treated with 50 μg·mL^{-1} CDs (q), 100 μg·mL^{-1} CDs (r), 200 μg·mL^{-1} CDs (s) for 24 h, (t) basal OCR and (u) maximal OCR. Oligo=oligomycin A, FCCP=carbonyl cyanide-4(trifluoromethoxy)phenylhydrazone, AA=antimycin A, Rot=rotenone. Adapted with permission from Ref. [3]. Copyright 2018, Wiley-VCH.

result in a 79% degree of cleavage under the irradiation of L-CPL, which was higher than other light sources (Fig. 3m–s). This exploration provided a novel application for chiral QDs in biology, paving the way to using QDs in the domain of medicine or even for therapy[52]. Sun and coworkers introduced chiral ligands into aqueous solutions of $HgCl_2$ and Na_2S to synthesize chiral HgS QDs, which significantly improved their water solubility and cytocompatibility. Even at high concentrations (20 mg/mL), the QDs still exhibited non-toxicity, which provided a new choice for fluorescence probes[53]. Currently, with the development of chiral molecular design, chiral QDs have overcome their potential toxicity in the biomedical field, bringing the greatest advantage of chirality into play.

2.3 Chiral CDs

CDs are attractive due to their excellent biocompatibility, low toxicity, and uncomplicated and inexpensive synthesis methods. Introducing chirality into CDs will broaden their applicability in chiral recognition, chiral separation, asymmetric catalysis and chiral detection. However, unlike extensively

DOI: 10.52396/JUSTC-2022-0167
JUSTC, **2023**, 53(3): 0303

studied CDs, chiral CDs have been researched only in recent years[54]. The first synthesis of chiral carbon dots was reported by Vázquez-Nakagawa et al. in 2016 by reacting graphene quantum dots (GQDs) with enantiomerically pure (R) or (S)-2-phenyl-1-propanol in a three-step process (Fig. 4a)[55]. After that, researchers continued to focus on the fabrication of chiral CDs. Prato et al. disclosed a bottom-up method to prepare chiral CDs by microwave-hydrothermal synthesis, using arginine as the precursor and (R, R)- or (S, S)-1,2-cyclohexanediamine (CHDA) as the chiral surface precursor. The dependence of their optical activities on the chiral surface precursors was also investigated. Thereafter, chiral CDs were employed as the chiral origin to endow supramolecular porphyrin with chirality via electrostatic interactions (Fig. 4c–e), which provided possibilities for the development of chiral compounds[56].

Although great breakthroughs have been made, it is still difficult to design chiral CDs with tunable wavelengths. Siyu Lu's group first proposed an approach to synthesize red- and multicolor-emitting chiral CDs with a quantum yield (QY) over 50% without varying the temperature (Fig. 4f). The CDs were prepared from L-/D-tryptophan and o-phenylenediamine through a solvothermal method. Then, through supramolecular self-assembly, the organic gel and chiral CDs were united to prepare circularly polarized multicolor-emitting CDs, and more importantly, variable proportions of several color emissions could contribute to white CPL (Fig. 4j–k). The CD spectra showed that the chiral CDs with different colors were alike but were different from their chiral precursors. In addition to CD signals, the author also spoke of CPL with a g_{lum} value up to 10^{-2}, which was a great breakthrough compared with previous reports[57].

Nie et al. dissolved and heated L-/D-Cys, the sole reagents, through a hydrothermal process to obtain chiral N-S-doped CDs (N-S-CDs). This approach not only achieved high efficiency (>80%) but also resulted in a desired QY of 41.26%. It is worth mentioning that the pH dependence of the fluorescence emission intensity caused by carbonyl (amino)-related localized electronic states was characterized by fluorescence quenching at low pH, and with increasing pH, the PL emission recovered. The CD spectra results indicated that the L-CDs and D-CDs with corresponding CD activities displayed invertible pH-dependent features similar to the PL emission spectra. The study also revealed that L-CDs or D-CDs showed different influences on glycolysis, which provided a novel trend for the promising application of chiral CDs[3]. Chirality gives CDs a number of distinguishing features ranging from optics to electronics. At the same time, the design principle of CDs helps to transfer chirality from the molecular level to the nano level.

3 Applications

3.1 AD and PD

AD and PD are typical neurodegenerative diseases in which neuropathological lesions are related to the deposition of abnormal proteins[58]. Studies have shown that no therapy can halt the deterioration of PD effectively to date[59]. Timely diagnosis and blocking of Aβ peptide fibrillation are crucial for the control of neurodegenerative diseases.

As adjuvants at the nano- or subnano-scale have great potential application prospects in the field of disease detection and treatment, chiral nanomaterials with high *g*-factor values and low biological toxicity are of great significance to the development of biological technology. In 2014, Qu et al. synthesized two kinds of triple-helical dinuclear metallosupramolecular complexes (Fig. 5a). CD tests (Fig. 5b, c) showed that these complexes could inhibit the structural transition from Aβ1−40 to the β-sheet conformation[60], which first reported the enantioselective inhibition of Aβ aggregation and attracted the attention of applying chiral nanomaterials in the deposition of amyloid protein to ameliorate neurodegenerative diseases. Afterwards, Tang et al. designed and prepared Au NPs stabilized by L- and D-GSH. The extensive distribution of GSH transporters in the brain enabled GSH-covered Au NPs to permeate the blood–brain barrier, and the surface chirality as well as helix structure could enantioselectively prevent Aβ aggregation in vitro[61]. For the detection of neurodegenerative diseases, Liz-Marzán et al. used protein fibrils as templates to assemble chiral NPs via noncovalent interactions, resulting in a helical nanorod array and enhanced chiral optical signals. Protein fibrils were identified by chiral signals, while healthy brain samples exhibited no meaningful optical activities, providing a new way to detect PD[62]. In addition, Kuang et al. proposed a strategy to alleviate neurodegenerative disease using chiral NPs with strong CD characteristics to clear senescent microglial cells (Fig. 5d), providing a promising way to alleviate PD[35]. In addition to methods directly using chiral signals for detection, Xu et al. synthesized L/D-Pt@Au triangular nanorings (Fig. 5e–j) as a label-free surface-enhanced Raman spectroscopy (SERS) platform to detect Aβ fibrils with ultrahigh sensitivity, paving the way for the use of chiroplasmonic nanomaterials as ultrasensitive SERS substrates to diagnose diseases caused by protein misfolding in an early stage[25]. In addition to chiral metal nanomaterials, Jelinek et al. synthesized enantiomeric CDs modified with L-lysine or D-lysine. Compared with metal nanomaterials, CDs are more biocompatible, making them attractive in biological applications[63]. Kuang et al. also prepared chiral Au NPs with different helical directions, causing selective induction of senescent cell apoptosis under light, which provided a promising strategy for alleviating PD[35].

Chiral nanomaterials have potential application prospects for detecting amyloid deposition and preventing protein aggregation, offering a new research idea for the diagnosis and treatment of neurodegenerative diseases.

3.2 Diabetes

Diabetes is a common chronic disease, with over one hundred million people suffering from diabetes in China, and global morbidity is increasing each year[64]. More seriously, diabetes also causes vascular complications such as heart failure, resulting in disease exacerbation or even death. Diabetic kidney disease is also a frequent complication that affects the health and life of patients[65, 66]. Generally, type 1 and type 2 diabetes are the most common, and statistics note that more than 90% of established diabetes cases are type 2[67]. Nonethe-

DOI: 10.52396/JUSTC-2022-0167
JUSTC, **2023**, 53(3): 0303

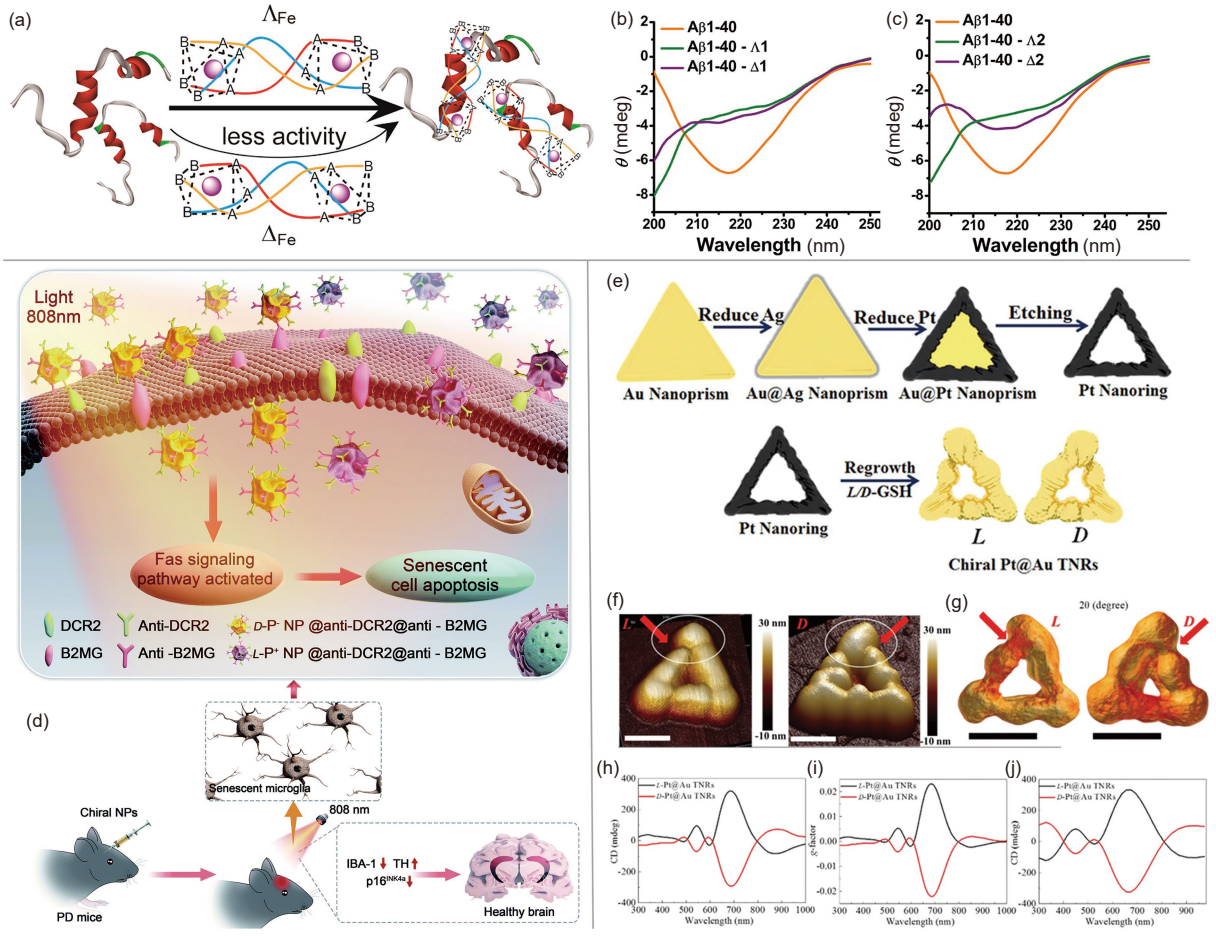

Fig. 5. (a) Representative illustration of enantioselective binding of Aβ by chiral metallosupramolecular complexes. CD spectra demonstrated the efficiency of (b) complex 1 and (c) complex 2 to inhibit Aβ1–40 aggregation. Adapted with permission from Ref. [55]. Copyright 2014, American Chemical Society. (d) Apoptosis pathways of senescent microglial cells in the brains of PD mice induced by chiral NPs. Adapted with permission from Ref. [32]. Copyright 2013, Royal Society of Chemistry. (e) Schematic illustration of the synthesis of chiral Pt@Au TNRs. (f) AFM and (g) 3D tomography images corresponding to L-Pt@Au TNR and D-Pt@Au TNR. (h) CD, (i) *g*-factor, and (j) simulated CD spectra of chiral Pt@Au TNRs. Adapted with permission from Ref. [22]. Copyright 2021, Wiley-VCH.

less, both type 1 and type 2 lead to disturbance of carbohydrate metabolism, which manifests as an excess of glucose[68]. In consideration of the prevalence of diabetes, precise and high-efficiency detection is highly desired.

Previous studies have shown that people suffering from diabetes produce higher levels of D-glucose and D-lactate[69], providing a new view to diagnose diabetes. However, it is still a major challenge to sensitively monitor the chirality in urine metabolites and establish the connection between diabetes and asymmetric metabolites. As a promising material, chiral plasma nanostructures with superchiral fields would improve the sensitivity of chiral sensing. Zheng et al. proposed plasmonic Moiré chiral metamaterials (MCMs) to generate superchiral fields and microbubbles (Fig. 6a). Microbubbles accumulated in the sample to increase the concentration, and plasma enhanced the sensing ability. As a consequence, the sensitivity for the detection of chiral substances could be 10^7 times that of traditional chiral noble metal nanostructures, and the LOD was under 100 pmol/L. The degree of accuracy for the diagnosis of diabetes reached 84% with 10 μL samples. The CD spectra indicated that L-glucose contributed to redshifts for the left-handed MCMs (LHMCMs) and blueshifts for the right-handed MCMs (RHMCMs), but conversely, D-glucose caused inverse shifts for MCMs (Fig. 6b). The chirality of metabolites would be detected efficiently through the shift of CD spectra[70]. Ngeontae and coworkers synthesized chiral CdS QDs capped with cysteine or penicillamine (PA) for glucose detection. The mechanism of detection was that the reaction of glucose oxidase and glucose would produce H_2O_2 in the presence of dissolved oxygen, which could destroy the structure of chiral QDs[71].

In the treatment of diabetes, controlling the level of blood glucose is crucial. Kang and coworkers have noticed the superior performance of chiral CDs in diabetes therapy, and they used L- or D-glutamic acid (Glu) as the precursor to obtain CDs by electrochemical methods (Fig. 6c, d). With increasing reaction time, the optical activity would be tuned even to the opposite chirality (Fig. 6e). Maltase could hydrolyze maltose to two molecules of glucose, which resulted in elevated blood sugar levels. Therefore, CDs were employed to inhibit the hydrolysis rate of maltase. It has been found that CDs with reversed chirality from the raw reagent enhanced

DOI: 10.52396/JUSTC-2022-0167
JUSTC, **2023**, 53(3): 0303

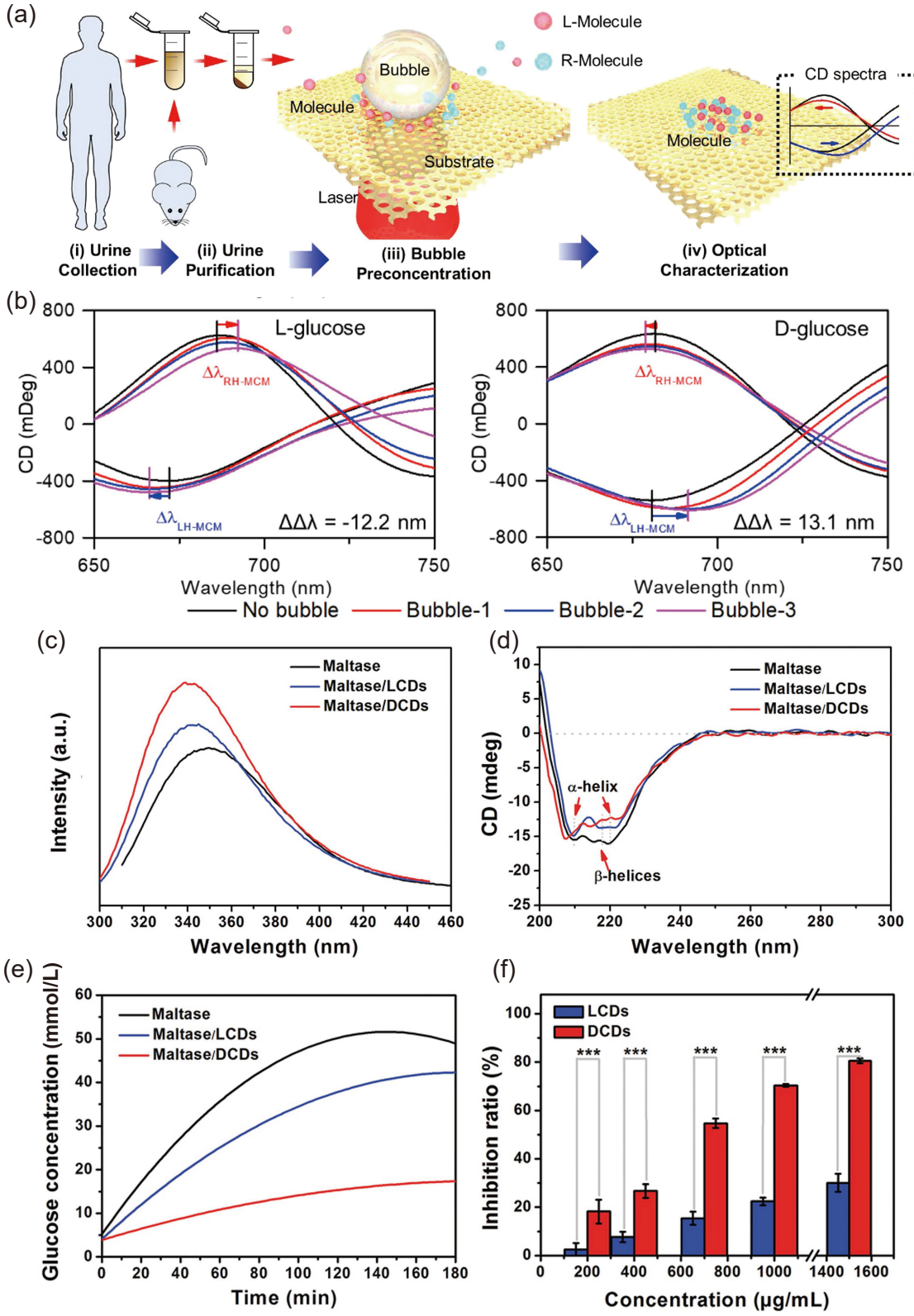

Fig. 6. (a) Illustration of the acquisition and purification of urine samples and the aggregation of chiral molecules in the urine on MCMs for more sensitive detection by the shift of CD spectra. (b) CD spectra of LH-MCMs and RH-MCMs under interaction with L- and D-glucose during continuous microbubble-assisted accumulation. Adapted with permission from Ref. [65]. Copyright 2021, American Chemical Society. (c) PL spectra (λ_{ex} = 280 nm) and (d) CD spectra of maltase (black line), maltase/LCDs (blue line), and maltase/DCDs (red line) with maltase and CD concentrations of 2.5 and 1.5 mg/mL, respectively. (e) Illustration of the effect of different hydrolysis times of maltase (black line), maltase/LCDs (blue line), and maltase/DCDs (red line) on the glucose concentration. (f) Illustration of the effect of LCDs and DCDs at different concentrations on the inhibition of maltase. Adapted with permission from Ref. [66]. Copyright 2019, Wiley-VCH.

DOI: 10.52396/JUSTC-2022-0167
JUSTC, **2023**, 53(3): 0303

the ability of DCDs to have a more powerful inhibitory effect on maltase activity, meaning that chirality could also exert an influence (Fig. 6f). This study not only developed a new application for CDs but also provided possibilities for diabetes treatment[72]. In addition, Qu et al. also studied how insulin and aβ cross-fibrillation were affected by the chirality of the interface surface to determine the pathological mechanisms, and they finally revealed that surface chirality could affect the cross oscillations of Aβ and insulin and the cytotoxicity of their aggregates[73].

3.3 Cancers

The incidence and mortality of malignant tumors are increasing worldwide, and it is important to detect the corresponding cancer markers. Abundant traditional techniques, such as immunohistochemical (IHC), fluorescent quantitation (qRT–PCR) and mass spectrometry (MS), have been developed to detect tumors. Unfortunately, these means were confronted with some pitfalls, such as high requirements for samples and high cost[22]. The introduction of chiral nanomaterials might alleviate this situation.

Currently, studies have demonstrated that lung cancer patients have high concentrations of serum alpha-fetoprotein (AFP), so liver cancer can be efficiently diagnosed by identifying the level of AFP[74]. Zhao et al. prepared Au NPs by the traditional citrate reduction process. With different [Au(III)]/[citrate] ratios, the size of the NPs was regulated. Subsequently, bis (p-sulfonatophenyl) phenylphosphine dihydrate dipotassium salt (BSPP) was employed to replace the original ligands for excellent dispersion prepared for DNA modification, and the original chirality was shown by the assembled dimer induced by DNA. To realize the specific determination of AFP, the AFP aptamer was introduced to interact with its complementary sequences. Once AFP was added, the powerful affinity between AFP and the AFP aptamer resulted in the destruction of Au NP dimers due to the decline in CD activity (Fig. 7c, d). It was considered that the CD intensity could be closely associated with the concentration of AFP, and both TEM and CD emerged to prove the log-linear variation between the CD intensity and the concentration of AFP in the range of 0.02 ng/mL to 5 ng/mL. Moreover, the LOD for AFP could reach 11 pg/mL, which is more sensitive compared to previous studies[75]. Xu and coworkers prepared a chiral Au@Ag dimer-based aptamer sensor for prostate-specific antigen (PSA), and the presence of Ag improved the

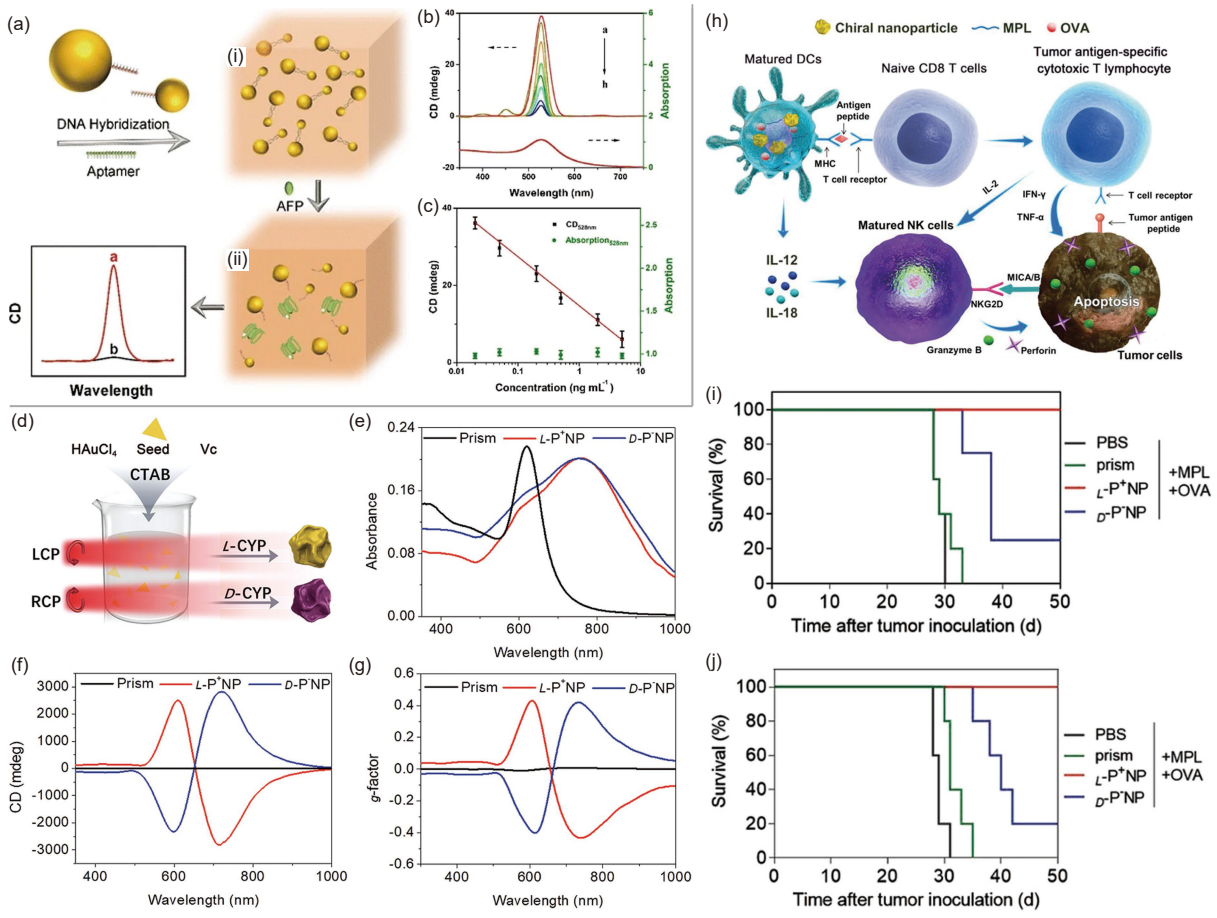

Fig. 7. (a) Illustration of the detection mechanism of chiral Au NPs for AFP. (b) CD and UV–vis spectra of chiral Au with different concentrations of AFP. (c) Illustration of the logarithmic relationship between CD spectra and the concentration of AFP. Adapted with permission from Ref. [68]. Copyright 2017, Springer Nature. (d) The fabrication process of chiral Au NPs. (e) UV–vis, (f) CD and (g) *g*-factor spectra of prism and chiral NPs under irradiation at 594 nm with 84 mW· cm^{-2} for 30 min. (h) The mechanism of action of chiral NPs for tumor therapy. (i) The survival of mice with tumor cells under the influence of PBS, prism, L-NPs and D-NPs. (j) The preventative effects. Adapted with permission from Ref. [34]. Copyright 2022, Wiley-VCH.

DOI: 10.52396/JUSTC-2022-0167
JUSTC, **2023**, 53(3): 0303

sensitivity and selectivity by inducing E-field enhancement (Fig. 7a). The interaction between PSA and the chiral sensor causes a change in the intensity of CD signals, which provides potential applications for cancer diagnosis[76].

In addition to detection, chiral nanostructures also offer promise in the application of cancer therapy. Immunotherapy is useful for cancer cure with low side effects and high efficiency by activating the body's immune system[77–79]. The implementation of immunotherapy is in contact with immunoreaction. $CD8^+$ T cells, also called cytotoxic T lymphocytes (CTLs), play a crucial role in immunity and can not only specifically identify cancer cells but also destroy them. In terms of antitumor activity, natural killer (NK) cells also exhibit important functions, even with higher efficiency for removing tumor cells (Fig. 7h). Kuang's group obtained chiral Au NPs with a maximal *g*-factor value of 0.44 through optically active compounds under polarized light (Fig. 7d–g). Next, the effects of chiral NPs on immunoreaction were explored, and the results indicated that compared with achiral NPs, chiral structures were more efficient in activating $CD8^+$ and NK cells. More importantly, L-Au NPs showed higher efficiency in inducing immunity, which made tumor cell apoptosis easier than D-NPs (Fig. 7i, j)[34]. In addition, the presence of chiral substances could also improve the effect of enzymes for the treatment of tumors. A chiral CD-glucose oxidase (GOx) nanoreactor was constructed by the coassembly of GOx and L/D-CD by Zheng et al., and L/D-GOx could significantly enhance the activity of GOx and improve the effective delivery of GOx to cancer cells[80].

4 Conclusions and perspectives

Chiral nanostructures are very significant for the detection, diagnosis and therapy of diseases, and many studies have explored them. To date, chirality has been introduced into inorganic materials; consequently, great advances have been achieved in the field. For example, chiral plasma materials with ideal *g*-factors as high as 0.44 emerged in 2022 and were used as immunologic adjuvants, and semiconductor nanostructures with controlled sizes and tunable optical properties were prepared more easily and efficiently. However, there are still many challenges that require researchers to study in more depth. First, chiral materials with higher asymmetry factors still need to be explored to put them better into practical applications. Second, the mechanism of the interaction between the inorganic core and surface ligands is unclear. In addition, biocompatibility, especially biodegradability and clearance from the body, is also a major problem before clinical trials.

Overall, the study of chiral inorganic materials for bioapplications is still in the primary stage. On the one hand, most chiral sensors are still in the experimental stage or even the theoretical level; on the other hand, the design of chiral materials is still relatively simple, which is not conducive to more cutting-edge and diversified bioapplications. With the development of clinical medicine, diagnosis is more accurate, and treatment is more efficient. However, the number of people suffering from AD, PD, diabetes or cancer is beyond the imagination. It is important to achieve early diagnosis and low-cost but effective treatment, and chiral materials are promising candidates, with lower LODs and greater accuracy.

Although several types of applications have been mentioned above, such as detection, diagnosis and therapy, considering the excellent properties of chiral materials, their applications in biology have no boundaries. In the future, the applications of CPL will come into view; for example, CPL-active semiconductor nanocrystals are widely known as ideal high-resolution markers for biological imaging and highly sensitive photosensitizers for therapy. Moreover, targeted therapy without loss of normal cells may occur with chiral materials, and chiral nanomaterials also provide a method for drug delivery vehicles. In addition, more chiral NPs that can be stimulated by NIR laser will be developed to improve tissue penetration and facilitate treatment. In short, from sample preparation to practical application exploration and basic research, much work remains to be done in the field of chirality in the future.

Acknowledgements

This work was supported by the National Key Research and Development Program of China (2021YFA1500400), the National Natural Science Foundation of China (22071226), the Funding of University of Science and Technology of China (KY2060000168, YD2060002013, KY2060000198), and the Collaborative Innovation Program of Hefei Science Center, CAS (CX2060000017).

Conflict of interest

The authors declare that they have no conflict of interest.

Biographies

Yaxin Wang is currently a graduate student under the supervision of Prof. Taotao Zhuang at the University of Science and Technology of China. Her recent research focuses on chiral nanomaterial-based films and related applications.

Zhi Tong is currently a graduate student under the supervision of Prof. Taotao Zhuang at the University of Science and Technology of China. Her recent research mainly focuses on the synthesis and bio-functions of chiral plasmonic nanomaterials.

Taotao Zhuang received his Ph.D. degree in Inorganic Chemistry from the University of Science and Technology of China and then worked as a postdoc fellow at the University of Toronto. He was appointed as a Professor at the University of Science and Technology of China in 2020. Now he is challenging to synthesize new inorganic chiral nanomaterials, understand the mechanism of structure–property, and realize the practical applications using home-made materials.

References

[1] Lebreton G, Géminard C, Lapraz F, et al. Molecular to organismal chirality is induced by the conserved myosin 1D. *Science,* **2018**, *362* (6417): 949–952.

[2] Tang K, Gan H, Li Y, et al. Stereoselective interaction between DNA and chiral surfaces. *J. Am. Chem. Soc.,* **2008**, *130* (34): 11284–11285.

[3] Li F, Li Y, Yang X, et al. Highly fluorescent chiral N-S-doped carbon dots from cysteine: Affecting cellular energy metabolism. *Angew. Chem. Int. Ed.,* **2018**, *57* (9): 2377–2382.

DOI: 10.52396/JUSTC-2022-0167
JUSTC, **2023**, 53(3): 0303

[4] Qu A, Sun M, Kim J Y, et al. Stimulation of neural stem cell differentiation by circularly polarized light transduced by chiral nanoassemblies. *Nat. Biomed. Eng.*, **2021**, *5* (1): 103–113.
[5] Li R S, Gao P F, Zhang H Z, et al. Chiral nanoprobes for targeting and long-term imaging of the Golgi apparatus. *Chem. Sci.*, **2017**, *8* (10): 6829–6835.
[6] Wang X, Wang M, Lei R, et al. Chiral surface of nanoparticles determines the orientation of adsorbed transferrin and its interaction with receptors. *ACS Nano*, **2017**, *11* (5): 4606–4616.
[7] Lee H E, Ahn H Y, Mun J, et al. Amino-acid- and peptide-directed synthesis of chiral plasmonic gold nanoparticles. *Nature*, **2018**, *556* (7701): 360–365.
[8] Wu C, Yin Y. Chiral semiconductor photonic thin film with tunable circularly polarized luminescence. *Matter*, **2022**, *5* (8): 2466–2468.
[9] Zheng H, Li W, Li W, et al. Uncovering the circular polarization potential of chiral photonic cellulose films for photonic applications. *Adv. Mater.*, **2018**, *30* (13): 1705948.
[10] Xu L, Xu Z, Ma W, et al. Highly selective recognition and ultrasensitive quantification of enantiomers. *J. Mater. Chem. B*, **2013**, *1* (35): 4478–4483.
[11] Fan H, Li K, Tu T, et al. ATP-induced emergent circularly polarized luminescence and encryption. *Angew. Chem. Int. Ed.*, **2022**, *61* (19): e202200727.
[12] Yan J, Yao Y, Yan S, et al. Chiral protein supraparticles for tumor suppression and synergistic immunotherapy: An enabling strategy for bioactive supramolecular chirality construction. *Nano Lett.*, **2020**, *20* (8): 5844–5852.
[13] Li S, Sun M, Hao C, et al. Chiral Cu_xCo_yS nanoparticles under magnetic field and NIR light to eliminate senescent cells. *Angew. Chem. Int. Ed.*, **2020**, *59* (33): 13915–13922.
[14] Miao J, Cai Y, Shao Y N, et al. Multiple cell death pathways triggered by temperature-mediated synergistic effect derived from chiral phototheranostic ablation nanoagents. *Appl. Mater. Today*, **2021**, *23*: 101001.
[15] Ma W, Hao C, Sun M, et al. Tuning of chiral construction, structural diversity, scale transformation and chiroptical applications. *Mater. Horiz.*, **2018**, *5* (2): 141–161.
[16] Wang Y, Xia Y. Near-infrared optically active $Cu_{2-x}S$ nanocrystals: Sacrificial template-ligand exchange integration fabrication and chirality dependent autophagy effects. *J. Mater. Chem. B*, **2020**, *8* (35): 7921–7930.
[17] Xu L, Wang X, Wang W, et al. Enantiomer-dependent immunological response to chiral nanoparticles. *Nature*, **2022**, *601* (7893): 366–373.
[18] Zhao X, Xu L, Sun M, et al. Tuning the interactions between chiral plasmonic films and living cells. *Nat. Commun.*, **2017**, *8* (1): 2007.
[19] Li Y W, Miao Z W, Shang Z W, et al. A visible- and NIR-light responsive photothermal therapy agent by chirality-dependent MoO_{3-x} nanoparticles. *Adv. Funct. Mater.*, **2020**, *30* (4): 1906311.
[20] Wang G, Hao C, Chen C, et al. Six-pointed star chiral cobalt superstructures with strong antibacterial activity. *Small*, **2022**, *18* (39): 2204219.
[21] Yeom J, Guimaraes P P G, Ahn H M, et al. Chiral supraparticles for controllable nanomedicine. *Adv. Mater.*, **2020**, *32* (1): e1903878.
[22] Djunic I, Elezovic I, Marinkovic M, et al. Osteolytic lesions marker in multiple myeloma. *Med. Oncol.*, **2011**, *28* (1): 237–240.
[23] Dunn G P, Bruce A T, Ikeda H, et al. Cancer immunoediting: From immunosurveillance to tumor escape. *Nat. Immunol.*, **2002**, *3* (11): 991–998.
[24] Liu J, Yang L, Qin P, et al. Recent advances in inorganic chiral nanomaterials. *Adv. Mater.*, **2021**, *33* (50): 2005506.
[25] Wang G, Hao C, Ma W, et al. Chiral plasmonic triangular nanorings with SERS activity for ultrasensitive detection of amyloid proteins in Alzheimer's disease. *Adv. Mater.*, **2021**, *33* (38): 2102337.
[26] González-Rubio G, Mosquera J, Kumar V, et al. Micelle-directed chiral seeded growth on anisotropic gold nanocrystals. *Science*, **2020**, *368* (6498): 1472–1477.
[27] Han B, Shi L, Gao X, et al. Ultra-stable silica-coated chiral Au-nanorod assemblies: Core–shell nanostructures with enhanced chiroptical properties. *Nano Res.*, **2016**, *9* (2): 451–457.
[28] Hao C, Xu L, Sun M, et al. Chirality on hierarchical self-assembly of Au@AuAg yolk-shell nanorods into core-satellite superstructures for biosensing in human cells. *Adv. Funct. Mater.*, **2018**, *28* (33): 1802372.
[29] Wang W, Wu F, Zhang Y, et al. Boosting chiral amplification in plasmon-coupled circular dichroism using discrete silver nanorods as amplifiers. *Chem. Commun.*, **2021**, *57* (60): 7390–7393.
[30] Wu X, Xu L, Ma W, et al. Propeller-like nanorod-upconversion nanoparticle assemblies with intense chiroptical activity and luminescence enhancement in aqueous phase. *Adv. Mater.*, **2016**, *28* (28): 5907–5915.
[31] Zheng G, Bao Z, Pérez-Juste J, et al. Tuning the morphology and chiroptical properties of discrete gold nanorods with amino acids. *Angew. Chem. Int. Ed.*, **2018**, *57* (50): 16452–16457.
[32] Guo X R, Wu D, Li Y, et al. Ordering silver nanowires for chiroptical activity. *Sci. China Mater.*, **2022**, *65* (5): 1362–1368.
[33] Tan L, Yu S J, Jin Y, et al. Inorganic chiral hybrid nanostructures for tailored chiroptics and chirality-dependent photocatalysis. *Angew. Chem. Int. Ed.*, **2022**, *61* (24): e202112400.
[34] Wang W, Zhao J, Hao C, et al. The development of chiral nanoparticles to target NK Cells and $CD8^+$ T cells for cancer immunotherapy. *Adv. Mater.*, **2022**, *34* (16): 2109354.
[35] Xu Z, Qu A, Zhang H, et al. Photoinduced elimination of senescent microglia cells in vivo by chiral gold nanoparticles. *Chem. Sci.*, **2022**, *13* (22): 6642–6654.
[36] Li S, Xu L, Ma W, et al. Dual-mode ultrasensitive quantification of microRNA in living cells by chiroplasmonic nanopyramids self-assembled from gold and upconversion nanoparticles. *J. Am. Chem. Soc.*, **2016**, *138* (1): 306–312.
[37] Sun M, Hao T, Li X, et al. Direct observation of selective autophagy induction in cells and tissues by self-assembled chiral nanodevice. *Nat. Commun.*, **2018**, *9* (1): 4494.
[38] Yan W, Xu L, Xu C, et al. Self-assembly of chiral nanoparticle pyramids with strong R/S optical activity. *J. Am. Chem. Soc.*, **2012**, *134* (36): 15114–15121.
[39] Li C, Li S, Zhao J, et al. Ultrasmall magneto-chiral cobalt hydroxide nanoparticles enable dynamic detection of reactive oxygen species in vivo. *J. Am. Chem. Soc.*, **2022**, *144* (4): 1580–1588.
[40] Probst P T, Mayer M, Gupta V, et al. Mechano-tunable chiral metasurfaces via colloidal assembly. *Nat. Mater.*, **2021**, *20* (7): 1024–1028.
[41] Yuan A, Hao C, Wu X, et al. Chiral Cu_xOS@ZIF-8 nanostructures for ultrasensitive quantification of hydrogen sulfide in vivo. *Adv. Mater.*, **2020**, *32* (19): 1906580.
[42] Cai J, Hao C, Sun M, et al. Chiral shell core-satellite nanostructures for ultrasensitive detection of mycotoxin. *Small*, **2018**, *14* (13): 1703931.
[43] Mastroianni A J, Claridge S A, Alivisatos A P. Pyramidal and chiral groupings of gold nanocrystals assembled using DNA scaffolds. *J. Am. Chem. Soc.*, **2009**, *131*: 8455–8459.
[44] Han B, Zhu Z, Li Z, et al. Conformation modulated optical activity enhancement in chiral cysteine and au nanorod assemblies. *J. Am. Chem. Soc.*, **2014**, *136* (46): 16104–16107.
[45] Wu X, Xu L, Liu L, et al. Unexpected chirality of nanoparticle dimers and ultrasensitive chiroplasmonic bioanalysis. *J. Am. Chem. Soc.*, **2013**, *135* (49): 18629–18636.
[46] Zhao X, Xu L, Sun M, et al. Gold-quantum dot core-satellite assemblies for lighting up microRNA in vitro and in vivo. *Small*, **2016**, *12* (34): 4662–4668.
[47] Ben-Moshe A, Govorov A O, Markovich G. Enantioselective synthesis of intrinsically chiral mercury sulfide nanocrystals. *Angew. Chem. Int. Ed.*, **2013**, *52* (4): 1275–1279.

DOI: 10.52396/JUSTC-2022-0167
JUSTC, **2023**, 53(3): 0303

[48] Nakashima T, Kobayashi Y, Kawai T. Optical activity and chiral memory of thiol-capped CdTe nanocrystals. *J. Am. Chem. Soc.,* **2009**, *131* (30): 10342–10343.
[49] Song L, Wang S, Kotov N A, et al. Nonexclusive fluorescent sensing for L/D enantiomers enabled by dynamic nanoparticle-nanorod assemblies. *Anal. Chem.,* **2012**, *84* (17): 7330–7335.
[50] Cheng J, Hao J, Liu H, et al. Optically Active CdSe-dot/CdS-rod nanocrystals with induced chirality and circularly polarized luminescence. *ACS Nano,* **2018**, *12* (6): 5341–5350.
[51] Kuznetsova V A, Mates-Torres E, Prochukhan N, et al. Effect of chiral ligand concentration and binding mode on chiroptical activity of CdSe/CdS quantum dots. *ACS Nano,* **2019**, *13* (11): 13560–13572.
[52] Hao C, Gao R, Li Y, et al. Chiral semiconductor nanoparticles for protein catalysis and profiling. *Angew. Chem. Int. Ed.,* **2019**, *58* (22): 7371–7374.
[53] Yang F, Gao G, Wang J, et al. Chiral β-HgS quantum dots: Aqueous synthesis, optical properties and cytocompatibility. *J. Colloid Interf. Sci.,* **2019**, *537*: 422–430.
[54] Ru Y, Ai L, Jia T T, et al. Recent advances in chiral carbonized polymer dots: From synthesis and properties to applications. *Nano Today,* **2020**, *34*: 100953.
[55] Vázquez-Nakagawa M, Rodríguez-Pérez L, Herranz M A, et al. Chirality transfer from graphene quantum dots. *Chem. Commun.,* **2016**, *52* (4): 665–668.
[56] Đorđević L, Arcudi F, D'Urso A, et al. Design principles of chiral carbon nanodots help convey chirality from molecular to nanoscale level. *Nat. Commun.,* **2018**, *9* (1): 3442.
[57] Ru Y, Sui L, Song H, et al. Rational design of multicolor-emitting chiral carbonized polymer dots for full-color and white circularly polarized luminescence. *Angew. Chem. Int. Ed.,* **2021**, *60* (25): 14091–14099.
[58] Ross C A, Poirier M A. Protein aggregation and neurodegenerative disease. *Nat. Med.,* **2004**, *10*: S10–S17.
[59] Bloem B R, Okun M S, Klein C. Parkinson's disease. *The Lancet,* **2021**, *397* (10291): 2284–2303.
[60] Li M, Howson S E, Dong K, et al. Chiral metallohelical complexes enantioselectively target amyloid β for treating Alzheimer's disease. *J. Am. Chem. Soc.,* **2014**, *136* (33): 11655–11663.
[61] Hou K, Zhao J, Wang H, et al. Chiral gold nanoparticles enantioselectively rescue memory deficits in a mouse model of Alzheimer's disease. *Nat. Commun.,* **2020**, *11* (1): 4790.
[62] Kumar J, Eraña H, López-Martínez E, et al. Detection of amyloid fibrils in Parkinson's disease using plasmonic chirality. *Proc. Natl. Acad. Sci. U. S. A.,* **2018**, *115* (13): 3225–3230.
[63] Malishev R, Arad E, Bhunia S K, et al. Chiral modulation of amyloid beta fibrillation and cytotoxicity by enantiomeric carbon dots. *Chem. Commun.,* **2018**, *54* (56): 7762–7765.
[64] Beckman J A, Creager M A. Vascular complications of diabetes. *Circ. Res.,* **2016**, *118* (11): 1771–1785.
[65] The Lancet. Untangling the complications of diabetes. *The Lancet,* **2018**, *391* (10138): 2389.
[66] Pop-Busui R, Januzzi J L, Bruemmer D, et al. Heart failure: An underappreciated complication of diabetes. A consensus report of the american diabetes association. *Diabetes Care,* **2022**, *45* (7): 1670–1690.
[67] Bullard K M, Cowie C C, Lessem S E, et al. Prevalence of diagnosed diabetes in adults by diabetes type - United States, 2016. *MMWR Morb. Mortal. Wkly. Rep.,* **2018**, *67* (12): 359–361.
[68] Cole J B, Florez J C. Genetics of diabetes mellitus and diabetes complications. *Nat. Rev. Nephrol.,* **2020**, *16* (7): 377–390.
[69] Talasniemi J P, Pennanen S, Savolainen H, et al. Analytical investigation: Assay of D-lactate in diabetic plasma and urine. *Clin. Biochem.,* **2008**, *41* (13): 1099–1103.
[70] Liu Y, Wu Z, Kollipara P S, et al. Label-free ultrasensitive detection of abnormal chiral metabolites in diabetes. *ACS Nano,* **2021**, *15* (4): 6448–6456.
[71] Ngamdee K, Ngeontae W. Circular dichroism glucose biosensor based on chiral cadmium sulfide quantum dots. *Sensor. Actuat. B Chem.,* **2018**, *274*: 402–411.
[72] Zhang M, Wang H, Wang B, et al. Maltase decorated by chiral carbon dots with inhibited enzyme activity for glucose level control. *Small,* **2019**, *15* (48): 1901512.
[73] Du Z, Guan Y, Ding C, et al. Cross-fibrillation of insulin and amyloid β on chiral surfaces: Chirality affects aggregation kinetics and cytotoxicity. *Nano Res.,* **2018**, *11* (8): 4102–4110.
[74] Lin J H, Wei Z J, Mao C M. A label-free immunosensor based on modified mesoporous silica for simultaneous determination of tumor markers. *Biosens. Bioelectron.,* **2011**, *29* (1): 40–45.
[75] Zhao H, Bian S, Yang Y, et al. Chiroplasmonic assemblies of gold nanoparticles as a novel method for sensitive detection of alpha-fetoprotein. *Microchim. Acta,* **2017**, *184* (6): 1855–1862.
[76] Tang L, Li S, Xu L, et al. Chirality-based Au@Ag nanorod dimers sensor for ultrasensitive psa detection. *ACS Appl. Mater. Interfaces,* **2015**, *7* (23): 12708–12712.
[77] Martin H, Smith L, Tomlinson D. Multidrug-resistant breast cancer: Current perspectives. *Breast Cancer:Targets and Therapy,* **2014**, *6*: 1–13.
[78] Galon J, Bruni D. Tumor immunology and tumor evolution: Intertwined histories. *Immunity,* **2020**, *52* (1): 55–81.
[79] Jhunjhunwala S, Hammer C, Delamarre L. Antigen presentation in cancer: Insights into tumour immunogenicity and immune evasion. *Nat. Rev. Cancer,* **2021**, *21* (5): 298–312.
[80] Gao P, Chen S, Liu S, et al. Chiral carbon dots-enzyme nanoreactors with enhanced catalytic activity for cancer therapy. *ACS Appl. Mater. Interfaces,* **2021**, *13* (47): 56456–56464.

DOI: 10.52396/JUSTC-2022-0167
JUSTC, **2023**, 53(3): 0303